Clays and Clay Minerals, Vol. 68, No. 6:623–631, 2020

NAPROXEN/LAYERED DOUBLE HYDROXIDE COMPOSITES FOR TISSUE-ENGINEERING APPLICATIONS: PHYSICOCHEMICAL CHARACTERIZATION AND BIOLOGICAL EVALUATION

Marcela P. Bernardo[1] *, Bruna C.S. Rodrigues[1], Tamires D. de Oliveira[2], Adriana P.M. Guedes[2], Alzir A. Batista[2], and Luiz H.C. Mattoso[1]

[1]National Nanotechnology Laboratory for Agribusiness, Embrapa Instrumentation, Brazilian Agricultural Research Corporation, São Carlos, São Paulo, Brazil

[2]Department of Chemistry, Federal University of São Carlos, São Carlos, São Paulo, Brazil

Abstract—Injured bone tissues can be healed with bone grafts, but this procedure may cause intense pain to the patient. A slow and localized delivery of nonsteroidal anti-inflammatory drugs (NSAIDs) could help to reduce the pain without affecting bone regeneration. The objective of the present study was to use [Mg-Al]-layered double hydroxide (LDH) as a matrix for controlled release of sodium naproxen (NAP). This system could be applied in biomaterial formulations (such as bone grafts) to achieve a local delivery of naproxen. [Mg-Al]-LDH successfully incorporated up to 80% (w/w) of naproxen by the structural reconstruction route, with the [Mg-Al]-LDH interlayer space increasing by 0.55 nm, corresponding to the drug molecule size. The evaluation of the naproxen release kinetics showed that 40% of the drug was delivered over 48 h in aqueous medium (pH 7.4 ± 0.1), indicating the potential of [Mg-Al]-LDH/NAP for local release of naproxen at adequate concentrations. Kinetic modeling showed that the naproxen release process was closely related to the Higuchi model, which considers the drug release as a diffusional process based on Fick's law. The chemical stability of NAP after the release tests was verified by ^{1}H NMR. The [Mg-Al]-LDH/NAP also exhibited low cytotoxicity toward fibroblast cells (L929 cell line), without modifications in their morphology and adhesion capacity. These results describe a suitable approach for preparing efficient systems for local delivery of nonsteroidal anti-inflammatory drugs for biomedical applications.

Keywords—Biomaterials · Controlled release · Cytotoxicity · Hydrotalcite · NSAID · Structural reconstruction

INTRODUCTION

Recent years have witnessed remarkable growth in the use of implanted medical devices, including joint replacements, dental implants, and bone grafts. Adverse reactions to grafts, such as device-mediated inflammation, fibrosis, coagulation, and infection are observed frequently, unfortunately (Tang and Eaton 1995). Nonsteroidal anti-inflammatory drugs are the most commonly used medications for pain relief in the world due to their blocking enzymes related to the inflammatory response in different tissues, mostly inhibiting the synthesis of prostaglandin (Cavalla et al. 2018). Several prostaglandins are essential for bone tissue regeneration after bone graft implantation. The NSAIDs play important roles in bone growth, affecting the formation of new tissues, particularly around the prostheses. The NSAIDs also stimulate the synthesis of collagen, which is beneficial for soft-tissue healing (Dahners and Mullis 2004). In this sense, the administration of NSAIDs at precise doses with local delivery could be effective in diminishing the pain caused by the graft implantation, while stimulating bone tissue regeneration (Vielpeau and Joubert 1999; Souza et al. 2018).

Naproxen is the dextrorotatory isomer of 6-methoxy-α-methyl-2-naphthalene acetic acid, which has been reported as the most effective drug for preventing disorientated bone formation around prostheses and after arthroplasty procedures (Brogden et al. 1975). For a successful drug-based therapy, the desired pharmacological response must be obtained at the specific site of action without harmful side effects (Wei et al. 2004). Some of the most common clinical effects related to the extensive oral administration of naproxen are related mainly to gastrointestinal complications caused by tissue damage, including gastroduodenal erosions and ulcerations, known as NSAID-induced gastropathy (Richy et al. 2004). The long-term administration of naproxen may cause these complications without extending the benefits (Lichtenstein et al. 1995). Slow-delivery systems are an excellent alternative to deliver drugs to target tissues at a controlled rate to provide the correct dosage, while delivery to other tissues is minimized or prevented (Khan et al. 2001). The incorporation of systems able to deliver NSAIDs, such as naproxen, in biomaterials, such as bone grafts, could overcome the deleterious side effects related to oral drug administration and also improve the drug effect in the graft implanted site.

Recently, LDHs have attracted much attention in drug delivery because of their biocompatibility, anion exchange properties, and nontoxicity (Hou and Jin 2007). LDHs are a family of layered materials with general stoichiometry $[M^{2+}_{1-x}M^{3+}_{x}(OH)_2]^{x+}(A^{n-})_{x/n}{\cdot}yH_2O$, where M^{2+} are bivalent cations, such as Ni^{2+}, Co^{2+}, Cu^{2+}, Zn^{2+}, and Ca^{2+}, and M^{3+} are trivalent cations, such as Al^{3+}, Cr^{3+}, Fe^{3+}, and Ga^{3+}. A^{n-} is a charge-balancing anion, and x is the

* E-mail address of corresponding author: marcelapiassib@gmail.com
DOI: 10.1007/s42860-020-00101-w

Electronic supplementary material The online version of this article (https://doi.org/10.1007/s42860-020-00101-w) contains supplementary material, which is available to authorized users.

molar ratio [$M^{3+}/(M^{3+} + M^{2+})$] ranging from 0.1 to 0.5 (Bernardo et al. 2017). The LDH crystalline structure consists of positively charged brucite ($Mg(OH)_2$)-like lamellae, in which trivalent cations isomorphically replace divalent cations at the octahedral sites (Reichle 1986).

Various anions have been intercalated in LDH, from simple inorganic anions, such as phosphate for agricultural applications (Bernardo et al. 2016), to functional biological molecules, such as vitamins (Fayyazbakhsh et al. 2017), genetic material (Choy et al. 1999), and drugs (Li et al. 2009) for therapeutic proposes.

Several approaches have been used to intercalate NSAIDs in LDHs. A LDH containing ibuprofen and ketoprofen was synthesized by coprecipitation (Rojas et al. 2014). Using the same methodology, fenbufen was intercalated in a LDH by Li et al. (2004). Diclofenac, gemfibrozil, ibuprofen, naproxen, 2-propylpen-tanoic acid, 4-biphenylacetic acid, and tolfenamic acid were intercalated into a [Li-Al]-LDH by ion exchange. Although these approaches provided interesting outcomes, the structural reconstruction has been poorly explored for naproxen intercalation (Del Arco et al. 2004; Berber et al. 2008; Hou and Jin 2007). This route is based on the calcination of LDH (>500°C) and subsequent stirring of the resulting mixed oxide in aqueous solution containing the anion to be intercalated (Rives et al. 2013). The mixed oxide then rehydrates, reconstructing the layered structure with the anion of interest intercalated. In addition, the controlled release of anti-inflammatory drugs from [Mg-Al]-LDH has been reported; the mechanisms and the impact of the released drug concentration on biological systems (*e.g.* in vitro studies) has rarely been investigated, however, especially for biomedical applications (Mondal et al. 2016).

Inspired by the above considerations, the present study aimed to investigate the intercalation of naproxen in a LDH to obtain a biocompatible system for local release of NSAIDs for biomedical applications. A reversible intercalation of naproxen in the [Mg-Al]-LDH through the reconstruction method was reported. The naproxen release profile and the cytotoxic properties of the [Mg-Al]-LDH/NAP system were also evaluated.

MATERIALS AND METHODS

Materials

Hydrotalcite-like LDH, sodium naproxen, and 3-(4,5-dimethylthiazol-2-yl)-2,5-diphenyltetrazolium bromide (MTT) were acquired from Sigma-Aldrich (St. Louis, Missouri, USA). Dulbecco's modified Eagle medium (DMEM) was purchased from Vitrocell (Campinas, São Paulo, Brazil). All reagents were used as received. Decarbonated ultra-pure H_2O ($\rho = 18.2$ MΩ cm) obtained by a Milli-Q system (Barnstead Nanopure Diamond, Thermo Fisher Scientific Inc., Dubuque, Iowa, USA) was used exclusively in all the experimental procedures.

Intercalation of Naproxen in Hydrotalcite-like LDH

Sodium naproxen (NAP, Fig. 1) was incorporated into the hydrotalcite-like LDH ([Mg-Al]-LDH) samples by the structural reconstruction method. The experimental conditions were

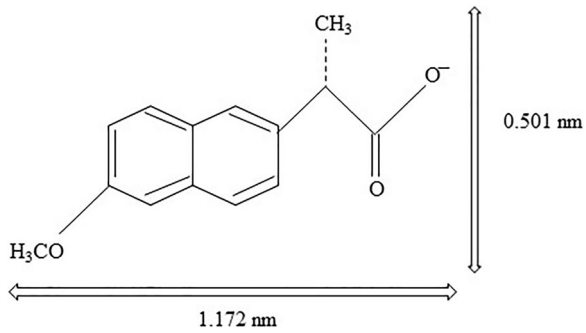

Fig. 1. Molecular size of naproxen molecule (after Carriazo et al. 2010)

established previously (Bernardo et al. 2016). Briefly, the [Mg-Al]-LDH samples were thermally treated at 600°C for 4 h. Subsequently, 100 mg of the calcined product was added to 50 mL of five different NAP solutions prepared with decarbonated water (1.0 g L^{-1}; 1.2 g L^{-1}; 1.8 g L^{-1}; 2.5 g L^{-1}; and 3.0 g L^{-1} or molar ratios of (NAP/[Mg-Al]-LDH): 1.21; 1.46; 2.21; 3.09; and 3.71, respectively) at 25°C, pH 8.1, under continuous agitation. After 24 h, the samples were centrifuged at 11.200×*g* for 10 min. Intercalated samples were then labeled as Mg-Al-LDH/NAP. The [Mg-Al]-LDH was also reconstructed in ultrapure water and used as a control.

Release Kinetics of Naproxen from [Mg-Al]-LDH/NAP

The desorption kinetics of NAP were studied at 25°C using water with pH 7.4 (± 0.1) as a standard medium. Briefly, masses of each Mg-Al-LDH/NAP sample equivalent to 11 mg of NAP were immersed in 40 mL of medium with continuous stirring for 48 h. Aliquots were taken at different times and centrifuged at 11,200×*g* for 10 min to determine the concentration of NAP in the supernatant by UV-Vis absorption spectroscopy (λ = 500–190 nm).

The drug-release data were analyzed using the Higuchi model (Eq. 1), which considers diffusion as the rate-determining step of the release process, and the zero order model (Eq. 2) associated with surface reaction kinetics (Lobo and Costa 2001).

$$M_t/M_\infty = \mathrm{k}_H t^{1/2} \quad (1)$$

$$M_t/M_\infty = \mathrm{k}t \quad (2)$$

where, M_t/M_∞ is the fraction of released drug at a time t and k is the kinetic release constant.

Cell Culture, Morphology Evaluation, and Toxicity Assay by MTT

Fibroblast cells (L929, ATCC: CCL 1) were cultivated at 37°C under humidified 5% CO_2 atmosphere in Dulbecco's modified Eagle medium (DMEM) supplemented with 10% (v/v) of fetal bovine serum (FBS). For the cytotoxicity assay, cells were seeded at a density of 1.5×10^4 cells per well and stored for 24 h for cell adhesion and the colorimetric method by MTT assay was performed (Mosmann 1983). After the

https://doi.org/10.1007/s42860-020-00101-w Published online by Cambridge University Press

incubation time, the aliquots from the release test (from each [Mg-Al]-LDH/NAP sample) were added individually to the cultivated cells and incubated for 48 h (37°C and 5% CO_2 atmosphere). Afterward, the MTT reagent was added and the cells were incubated again for 4 h at the same conditions. The formazan crystals were solubilized in isopropanol and the absorbance was determined at 540 nm in a microplate reader (Biotek Epoch, Winooski, Vermont, USA). All experiments were repeated three times using four well replicates each time. The software *GraphPad Prism* was used for data processing.

For the morphological assay, the fibroblast cells were seeded at a density of 8×10^4 cells per well and stored for 24 h at the same conditions. Then, the aliquots from the release test (from each NAP-loaded Mg-Al-LDH sample) were added individually and the cell morphology was registered at different times (0, 24, and 48 h) using an inverted microscope (Nikon Eclipse TS100- Melville, New York, USA) attached to a Motcam 1SP 1.3 MP camera (Hong Kong).

Characterizations

Powder X-ray diffraction (PXRD) measurements were conducted on a Shimadzu (Kyoto, Japan) XRD 6000 diffractometer using Ni-filtered CuKα radiation (λ = 1.5405 Å). The PXRD patterns were taken over the range 5–70°2θ with a scanning speed of 2°2θ min^{-1}. Interplanar spaces were calculated using Bragg's law. Attenuated total reflectance Fourier-transform infrared (ATR-FTIR) analyses were performed on a Bruker VERTEX 70 spectrometer (Billerica, Massachusetts, USA) using a spectral resolution of 2 cm^{-1} and 32 scans. Sample morphology was investigated with a field emission scanning electron microscope (FE-SEM) Supra 35-VP Carl Zeiss (Oberkochen, Germany) operating at 15 kV. Thermal degradation was evaluated using a TGA Q500 thermogravimetric analyzer (TA Instruments, New Castle, Delaware, USA) running with a N_2 atmosphere (60 mL·min^{-1}) from 25 to 800°C at a heating rate of 10°C·min^{-1}. To evaluate the integrity of the naproxen molecule after the release process, ^{1}H NMR spectra were obtained using a Bruker Avance III DRX-400 spectrometer (Billerica, Massachusetts, USA) at 9.4 T using D_2O as a solvent.

RESULTS AND DISCUSSION

Structural and Morphological Characterization

The structural reconstruction of [Mg-Al]-LDH was evaluated by a series of PXRD measurements (Fig. 2i). The PXRD pattern of [Mg-Al]-LDH in Fig. 2iA corresponds to the hexagonal lattice with rhombohedral 3R symmetry, with basal spacing (d_{003}) of 0.76 nm, which is typical of hydrotalcite (Cavani et al. 1991). After thermal treatment at 600°C, the original [Mg-Al]-LDH structure was altered completely; only reflections ascribed to the oxides of the constituent metals remained, indicating the total collapse of the LDH layered structure (Fig. 2iB). Once in contact with pure water, the three-dimensional layered structure was restored, as shown in the PXRD pattern in Fig. 2iC.

The intercalation of naproxen between the [Mg-Al]-LDH layers is the first step to guarantee its controlled and localized delivery. When the calcined material was put in contact with the naproxen solutions (Fig. 2iiD–H), the characteristic reflections of LDH were still observed, indicating that a large proportion of the [Mg-Al]-LDH particles was restored even in the presence of naproxen. A reflection observed at ~43.4°2θ, related to the MgO phase, was probably due to the fraction of non-reconstructed and calcinated [Mg-Al]-LDH, however. Note that the intensity of this reflection increased with the naproxen concentration, suggesting that naproxen inhibits the reconstruction of [Mg-Al]-LDH.

On the other hand, as the initial naproxen concentration was increased, the (003) reflection shifted to lower angles, with increase in the *d* spacing (according to Bragg's law), indicating that the naproxen molecules were partially intercalated into the LDH interlayer space (Table 1). After subtraction of the brucite-like layer width (0.48 nm), the gallery height, on average, was 0.55 nm, which matches the naproxen molecular size (1.172 nm×0.501 nm), according to Carriazo et al. (2010). This

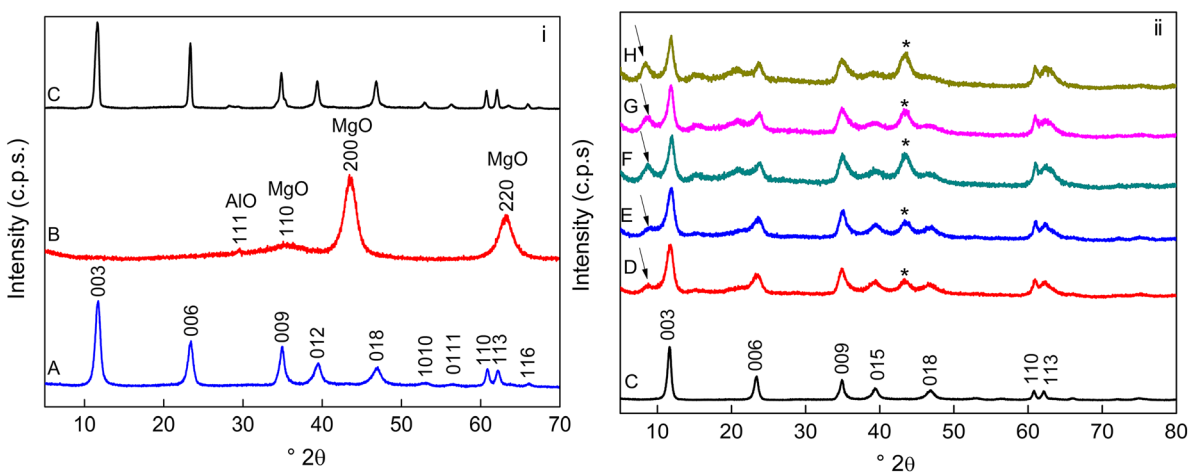

Fig. 2. PDRX of (**i**): commercial [Mg-Al]-LDH reconstructed in pure water (A); calcined [Mg-Al]-LDH (B); and reconstructed [Mg-Al]-LDH (C). (**ii**) PXRD of commercial [Mg-Al]-LDH intercalated with naproxen at various initial concentrations: 1.0 g L^{-1} (D); 1.2 g L^{-1} (E); 1.8 g L^{-1} (F); 2.5 g L^{-1} (G); and (H) 3.0 g L^{-1} (H). * MgO phase

https://doi.org/10.1007/s42860-020-00101-w Published online by Cambridge University Press

Table 1. Naproxen concentration after interaction with [Mg-Al]-LDH and the resulting interlayer space of [Mg-Al]-LDH

Initial concentration (g L^{-1})	Amount of NAPAdsorbed (g.g [Mg-Al]-LDH^{-1})	Interlayer space (nm)
[Mg-Al]-LDH	-	0.27
1.0	0.40	0.53
1.2	0.47	0.52
1.8	0.50	0.55
2.5	0.57	0.56
3.0	0.75	0.57

suggested that the naproxen molecules were intercalated in the LDH galleries as a monolayer with their aromatic rings parallel to the brucite-like layers, and their carboxylic groups interacting with the layers through electrostatic interactions (Del Arco et al. 2004), as represented schematically in Fig. 3. The increase in the d_{003} spacing is followed by the increase in the amount of naproxen intercalated (Table 1), probably due to the increase in the driving force which overcomes all mass-transfer resistance of solutes between the solid and aqueous phases (Hasan et al. 2012). The presence of carbonate anions was noted due to the atmosphere conditions used in the intercalation reaction and also to the ubiquitous presence of CO_2 (Arco et al. 2004). The carbonate anions help to stabilize the LDH structure and, because of its atoxicity, naproxen-loaded [Mg-Al]-LDH is no less suitable as a delivery system for biomedical applications.

ATR-FTIR spectra provided insights into the interactions between naproxen and [Mg-Al]-LDH (Fig. 4). Naproxen exhibited a large number of bands due to the various functional groups in its molecule. Several bands in the range of 1631–1459 cm^{-1} are due to υ(C–C) modes of aromatic groups. The δ(CH_3) band is recorded at 1398 cm^{-1}, the modes υ(CO), υ(C–O–C), and δ(CH_3) are registered at 1265, 1162, and 1000 cm^{-1}, respectively (Rojas et al. 2014). On the other hand, the typical bands of [Mg-Al]-LDH occur above 1350 cm^{-1}, indicating the presence of CO_3^{2-}; the bands at 650, 550, and 450 cm^{-1} are related to the metal–oxygen vibrations (Bernardo and Ribeiro 2018). The spectra of the NAP-loaded [Mg-Al]-LDH showed that the bands at 1585 cm^{-1} and 1396 cm^{-1}, related to asymmetric and symmetric vibrations of υ(COO^-), were shifted to 1547 cm^{-1} and 1365 cm^{-1}, respectively, indicating chemical interactions between naproxen and the LDH layers (Del Arco et al. 2004). In addition to the intercalation process, the naproxen molecules interacted with the [Mg-Al]-LDH layer external surface by electrostatic interactions (Yang et al. 2014).

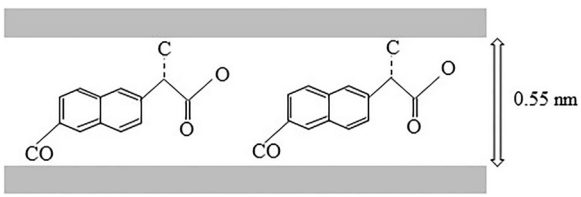

Fig. 3. Schematic diagram showing naproxen interaction with the brucite-like layers of [Mg-Al]-LDH

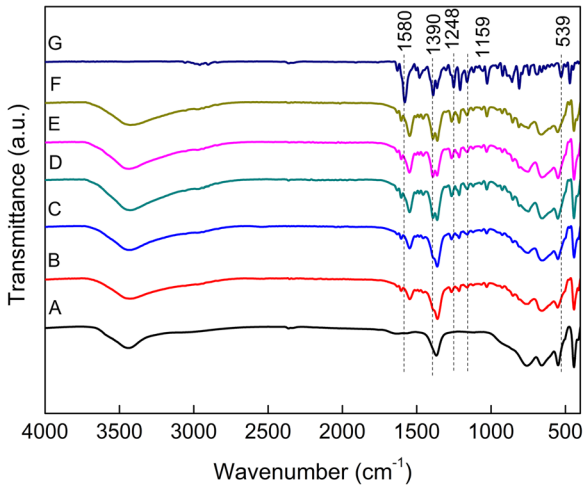

Fig. 4. ATR-FTIR spectra of (A) commercial [Mg-Al]-LDH, [Mg-Al]-LDH/NAP samples obtained from various initial naproxen concentrations, (B) 1.0 g L^{-1}; (C) 1.2 g L^{-1}; (D) 1.8 g L^{-1}; (E) 2.5 g L^{-1}; (F) 3.0 g L^{-1}, and (G) pure naproxen

The morphology of LDH is an important factor for the release of intercalated components. The [Mg-Al]-LDH/NAP exhibited a typical hydrotalcite structure, composed of quasi-hexagonal layers, with plate-like morphology (Fig. 5). Regardless of the NAP concentration, the hexagonal structure was well maintained, reflecting a good crystallinity, as indicated by the XRD measurements. The intercalation of naproxen by structural reconstruction does not affect the LDH morphology, therefore (Costa et al. 2008). According to Huang et al. (2015), the LDH morphology changes during the release process due to the formation of drug aggregates at specific layer regions, which may influence the drug-release rate.

The thermal stability and further compositional data of the [Mg-Al]-LDH/NAP samples were assessed by thermogravimetric analysis (TGA) (Fig. 6). Overall, similar mass-loss events were found regardless of the amount of NAP adsorbed. The first mass-loss stage (25–60°C) was ascribed to desorption of surface water, as was also observed in the thermogravimetric profile of pure sodium naproxen (Supporting Information, Fig. S1). The second and third mass-loss stages (165–170°C and 280–350°C) are related to the removal of water adsorbed within the hydrotalcite layers, dehydroxylation of the hydrotalcite-like phase, and thermal decomposition of free naproxen, respectively (Bernardo and Ribeiro 2018). The thermal decomposition of naproxen occurs simultaneously with the LDH dehydroxylation; therefore, the mass-loss percentage was greater than the amount of naproxen in the samples (Menagen et al. 2017). Accordingly, the last mass-loss stage occurring above 550°C was associated with the evolution of CO_3^{2-} anions intercalated in the LDH galleries (Hussein et al. 2019).

In vitro Drug Release

After the proper intercalation of naproxen in the [Mg-Al]-LDH, evaluating the rate of drug release under conditions that could simulate real applications is essential. The naproxen release profiles for all the [Mg-Al]-LDH/NAP samples were

https://doi.org/10.1007/s42860-020-00101-w Published online by Cambridge University Press

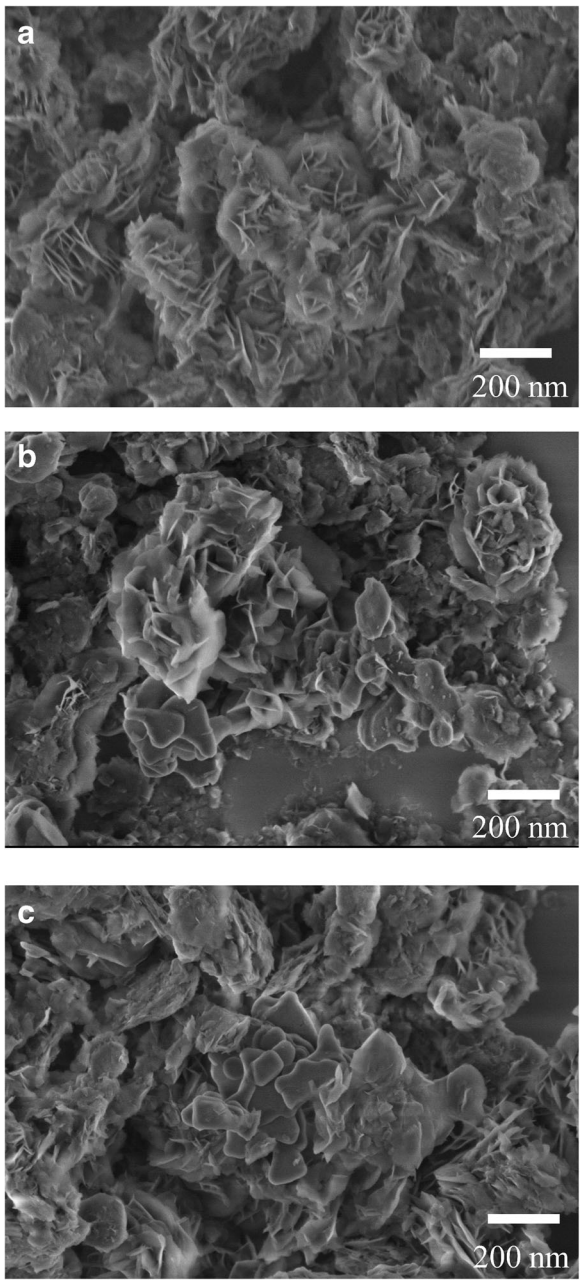

Fig. 5. SEM images of [Mg-Al]-LDH/NAP samples obtained from different initial naproxen concentrations: **a** 1.0 g L^{-1}; **b** 1.8 g L^{-1}, and **c** 3.0 g L^{-1}

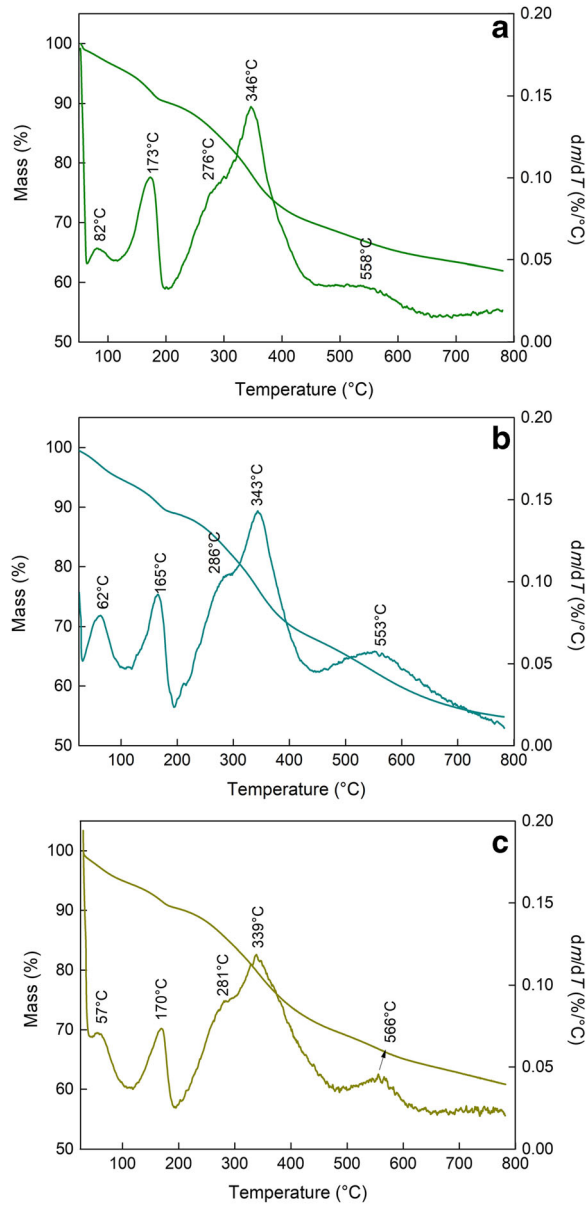

Fig. 6. Thermogravimetric (TG) and differential thermogravimetric (DTG) curves of [Mg-Al]-LDH/NAP samples obtained from various initial naproxen concentrations: **a** 1.0 g L^{-1}; **b** 1.8 g L^{-1}, and **c** 3.0 g L^{-1}

modified when compared with the free drug (Fig. 7A). The free naproxen is immediately solubilized, and its concentration is promptly available (Supporting Information, Fig. S2). [Mg-Al]-LDH delayed the naproxen release, which is very interesting because the nanolayers may protect the drug against physicochemical degradation and reduce adverse effects on non-target tissues, while providing the dose at an adequate frequency, improving the drug bioavailability and stimulating the regeneration of injured tissues (Mishra et al. 2018).

The [Mg-Al]-LDH matrix controlled the naproxen release effectively until 180 min. These results suggested that a small fraction of naproxen be ascribed to the external LDH particle surface. This delayed-release profile is desired for medical applications (Djaballah et al. 2018). After 3 h, all the samples exhibited an increase in the naproxen release rate. Note that the naproxen release rate was greater for the samples with less adsorbed naproxen, probably because of the presence of NAP in the layers. In particular, the naproxen molecules located at the layer edges could be released faster than the molecules

https://doi.org/10.1007/s42860-020-00101-w Published online by Cambridge University Press

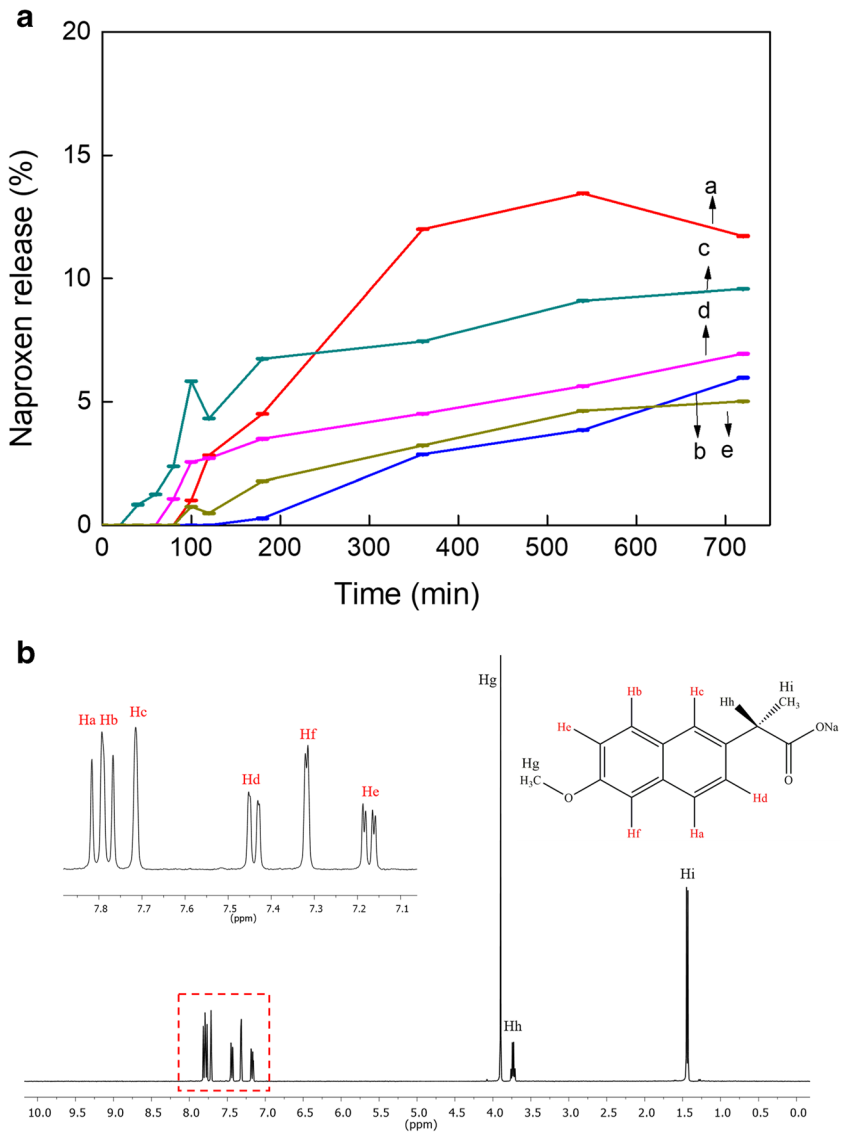

Fig. 7. **a** Kinetics of naproxen release in water (measurements in triplicate) for [Mg-Al]-LDH/NAP samples obtained from various initial naproxen concentrations (a) 1.0 g L^{-1}; (b) 1.2 g L^{-1}; (c) 1.8 g L^{-1}; (d) 2.5 g L^{-1}; and (e) 3.0 g L^{-1}. **b** ^{1}H NMR spectrum in D_2O of the release medium after 48 h. The aromatic region in the spectrum was expanded and is shown as an insert

intercalated in the LDH layers. The drug diffusion rate out of the LDH matrix is controlled by the layer rigidity and diffusion path length (Ambrogi et al. 2001). In this context, [Mg-Al]-LDH may be considered as a semi-rigid material (Dresselhaus 1986; Hines et al. 2000). In this kind of matrix, the interlayer distance decreases when large anions (such as naproxen) are replaced by small species (such as anions present in the aqueous medium). The exchange of a naproxen fraction, especially that adsorbed on the external LDH particle surface, caused a decrease in the interlayer distance and, as a consequence, the drug release rate decreased. In this case, a phase boundary is formed in the LDH crystals, where small and large interlayer distances co-exist. In other words, the external zone, where the naproxen was released, and the internal zone, in which naproxen is still intercalated, exist simultaneously. This phase boundary moves toward the central part of the LDH crystal and the release rate declines (Ambrogi et al. 2001). Due to the release conditions (water, pH 7.4), the presence of anions able to exchange with the naproxen molecules external to the [Mg-Al]-LDH crystal is limited, leading to a small dose being released. The release rate may be sustained over a prolonged period, however, until the formation of the phase boundary, achieving one of the most desired objectives of a controlled-release system.

Considering the application of the naproxen-loaded [Mg-Al]-LDH as a component of biomaterials (e.g. bone grafts), the amount of naproxen-loaded [Mg-Al]-LDH should be adjusted for the body weight of each patient. For example, the smallest naproxen dose for anti-inflammatory effect is 3 mg/kg (Davies et al. 1997). Considering the concentration of 0.4 g/g NAP/

https://doi.org/10.1007/s42860-020-00101-w Published online by Cambridge University Press

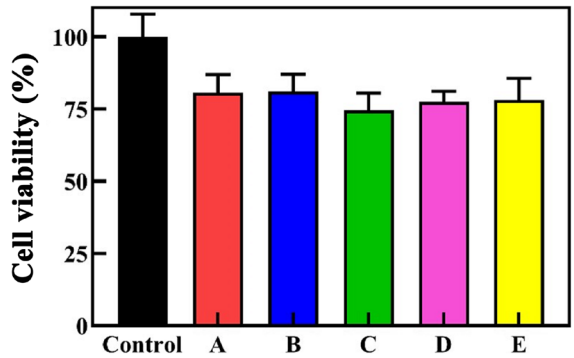

Fig. 8. Cell viability of L929 cell line before (control) and after 48 h incubation with the aqueous release media from [Mg-Al]-LDH/NAP samples obtained from various initial naproxen concentrations: (A) 1.0 g L^{-1}; (B) 1.2 g L^{-1}; (C) 1.8 g L^{-1}; (D) 2.5 g L^{-1}; and (E) 3.0 g L^{-1}

[Mg-Al]-LDH (sample 1 g/L), which showed a release of 39% after 48 h, the bone graft should have ~1.5 g of naproxen-loaded-[Mg-Al]-LDH. The fabrication of custom-designed grafts is becoming a reality, especially with the use of the 3D-printing technique (Mobbs et al. 2017). In fact, small doses of naproxen may be clinically useful in bone-tissue regeneration without harming the formation, healing, and remodeling of bones (Dahners and Mullis 2004).

Naproxen release kinetics were described by mathematical models. The results suggested that Higuchi's equation best described the release profile kinetics (Supporting Information, Table S1), which considers drug release as a diffusional process based on Fick's law. This indicates that anion exchange is the main mechanism in the release of naproxen from [Mg-Al]-LDH (Lobo and Costa 2001; Rojas et al. 2015).

Naproxen should maintain complete molecular integrity to guarantee its biological activity. ^{1}H NMR was performed on the aqueous medium used in the release experiments (after 48 h) to evaluate the structure of the released naproxen molecules. The ^{1}H NMR spectrum showed signals corresponding to pure naproxen, with aromatic signals at δ = 7.79 (2H, m), δ = 7.72 (1H, s), δ = 7.44 (1H, dd), δ = 7.32 (1H, d, J = 2.3 Hz), and δ = 7.17 (1H, dd) and methylene groups at δ = 3.90 (3H, s) and δ = 1.44 (3H, s), and finally, one aliphatic signal at δ = 3.74 (1H, m) (Fig. 7B). The spectrum of pure naproxen is shown in Supporting Information, Fig. S3. After this analysis, the naproxen molecules remained stable after adsorption and release from [Mg-Al]-LDH; thus they may play an anti-inflammatory role at the site of action.

Biological Evaluation

[Mg-Al]-LDH have been useful in biological applications, due to the low or null toxicity among several characteristics (Choy et al. 2007). Local drug delivery and the presence of LDH may cause variations at the site of action and deleterious consequences to cell growth, however. Biological evaluation is essential to guarantee the cell viability in the tissue regeneration process, however.

The medium used in the release tests of [Mg-Al]-LDH/NAP was examined for its cytotoxicity, concerning the relative cell viability (%) of fibroblast cells after 48 h of incubation (Fig. 8). The samples presented a low degree of cytotoxicity, regardless of the initial NAP concentration. This low cytotoxicity may be related to the [Mg-Al]-LDH, because the NAP concentration used in this study did not affect cell viability (Supporting Information, Fig. S4). According to Xu et al. (2007), the level of LDH cytotoxicity is variable for different cell lines. For the blood cell lines, a LDH concentration of 1000 μg/mL does not affect cell viability. On the other hand, concentrations as high as 500 μg/mL caused a 50% cell viability reduction in human embryonic kidney cells (Kriven et al. 2004). The LDH cytotoxicity mechanism is probably related to the cell membrane disruption due to the binding of

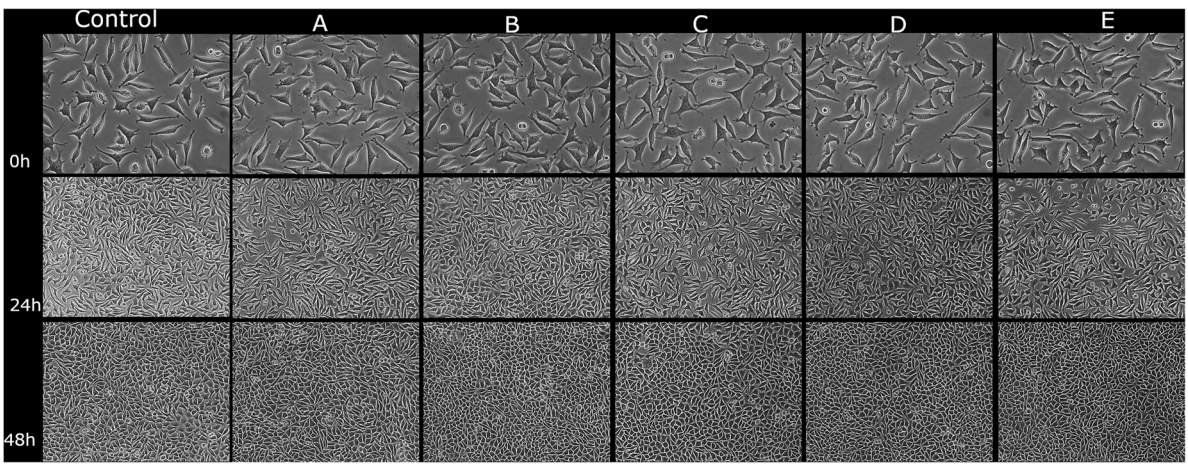

Fig. 9. Morphological evaluation of L929 cells before (control) and after 0, 24, and 48 h of incubation with the aqueous release medium from [Mg-Al]-LDH/NAP samples obtained from various initial naproxen concentrations: (A) 1.0 g L^{-1}; (B) 1.2 g L^{-1}; (C) 1.8 g L^{-1}; (D) 2.5 g L^{-1}; and (E) 3.0 g L^{-1}

https://doi.org/10.1007/s42860-020-00101-w Published online by Cambridge University Press

the cell surface by the LDH positive charges, which interrupt normal cell function, leading to apoptosis (Rhaese et al. 2003).

Despite the low cytotoxicity, the fibroblast cells maintained the specific cell morphology for 48 h, regardless of the naproxen concentration in the medium, in comparison with the control group (Fig. 9). After 48 h, the cells kept their capacity to adhere and proliferate on the surface of a cultivation plate. This means that the cells were attached and alive, demonstrating the biocompatibility and low cytotoxicity of the [Mg-Al]-LDH/NAP samples, which is expected to be vital in the fine-tuning of this low-dose delivery system.

CONCLUSIONS

The structural reconstruction method allowed for efficient intercalation of naproxen in [Mg-Al]-LDH. The increase in the interlayer space suggested a parallel orientation of the naproxen aromatic rings between the brucite-like LDH layers. The typical hexagonal structure of [Mg-Al]-LDH was maintained after naproxen adsorption, regardless of the initial drug concentration. Kinetic studies revealed a slow naproxen release, explained mainly by the rigidity of the LDH matrix. Also, the naproxen release kinetics were described well by the Higuchi model, which considers the release a diffusional process based on Fick's law. The samples demonstrated low cytotoxicity toward fibroblast cells (L929 cell line) without modifications in the morphology and adhesion capacity of the cells. Therefore, [Mg-Al]-LDH is a good host matrix for local delivery of naproxen, demonstrating a great potential for biomedical applications by assisting in reduction of pain intensity and, at the same time, allowing for tissue regeneration.

ACKNOWLEDGMENTS

The authors are grateful to Embrapa Instrumentation for laboratory support and for financial support from FAPESP (grant n°. 2018/07860-9), CNPq, and SISNANO/MCTI.

Funding

Funding sources are as stated in the Acknowledgments.

Compliance with Ethical Statements

Conflict of Interest

The authors declare that they have no conflict of interest.

REFERENCES

Ambrogi, V., Fardella, G., Grandolini, G., & Perioli, L. (2001). Intercalation compounds of hydrotalcite-like anionic clays with antiinflammatory agents – I. Intercalation and in vitro release of ibuprofen. *International Journal of Pharmaceutics, 220*, 23–32. https://doi.org/10.1016/S0378-5173(01)00629-9.

Arco, M. del, Rrez, S. G., Martı, C., Rives, V., & Rocha, J. (2004). Synthesis and characterization of layered double hydroxides (LDH) intercalated with non-steroidal anti-inflammatory drugs (NSAID). *Journal of Solid State Chemistry*, *177*, 3954–3962. https://doi.org/10.1016/j.jssc.2004.08.006

Berber, M. R., Minagawa, K., & Katoh, M. (2008). Nanocomposites of 2-arylpropionic acid drugs based on Mg – Al layered double hydroxide for dissolution. *European Journal of Pharmaceutical Sciences, 5*, 354–360. https://doi.org/10.1016/j.ejps.2008.08.006.

Bernardo, M. P., Moreira, F. K. V., Colnago, L. A., & Ribeiro, C. (2016). Physico-chemical assessment of [Mg-Al-PO_4]-LDHs obtained by structural reconstruction in high concentration of phosphate. *Colloids and Surfaces A: Physicochemical and Engineering Aspects, 497*, 53–62. https://doi.org/10.1016/j.colsurfa.2016.02.021.

Bernardo, M. P., Moreira, F. K. V., & Ribeiro, C. (2017). Synthesis and characterization of eco-friendly Ca-Al-LDH loaded with phosphate for agricultural applications. *Applied Clay Science, 137*, 143–150. https://doi.org/10.1016/j.clay.2016.12.022.

Bernardo, M. P., & Ribeiro, C. (2018). [Mg-Al]-LDH and [Zn-Al]-LDH as matrices for removal of high loadings of phosphate. *Materials Research, 21*, 1–9. https://doi.org/10.1590/1980-5373-MR-2017-1001.

Brogden, R. N., Finder, R. M., Sawyer, P. R., Speight, T. M., & Avery, G. S. (1975). Naproxen: A review of its pharmacological properties and therapeutic efficacy and use. *Drugs, 9*, 326–363. https://doi.org/10.2165/00003495-197509050-00002.

Carriazo, D., del Arco, M., Martín, C., Ramos, C., & Rives, V. (2010). Influence of the inorganic matrix nature on the sustained release of naproxen. *Microporous and Mesoporous Materials*, *130*, 229–238. https://doi.org/10.1016/j.micromeso.2009.11.014

Cavalla, F., Biguetti, C. C., Garlet, T. P., Trombone, A. P. F., & Garlet, G. P. (2018). Inflammatory pathways of bone resorption in periodontitis. Pp. 59–86 in: *Pathogenesis of Periodontal Diseases* (G. N. B. N. Bostanci, editor). https://doi.org/10.1007/978-3-319-53737-5

Cavani, F., Trifirò, F., & Vaccari, A. (1991). Hydrotalcite-type anionic clays: Preparation, properties and applications. *Catalysis Today, 11*, 173–301. https://doi.org/10.1016/0920-5861(91)80068-K.

Choy, J., Kwak, S., Park, J., & May, R. V. (1999). intercalative nanohybrids of nucleoside monophosphates and DNA in layered metal hydroxide. *Journal of the American Chemical Society, 121*, 1399–1400.

Choy, J. H., Choi, S. J., Oh, J. M., & Park, T. (2007). Clay minerals and layered double hydroxides for novel biological applications. *Applied Clay Science, 36*, 122–132. https://doi.org/10.1016/j.clay.2006.07.007.

Costa, F., Saphiannikova, M., Wagenknecht, U., & Heinrich, G. (2008). Layered double hydroxide based polymer nanocomposites. Pp. 101–168 in: *Wax Crystal Control · Nanocomposites · Stimuli-Responsive Polymers*. Advances in Polymer Science, vol 210. Springer, Berlin, Heidelberg. https://doi.org/10.1007/12_2007_123

Dahners, L. E., & Mullis, B. H. (2004). Effects of nonsteroidal anti-inflammatory drugs on bone formation and soft-tissue healing. *The Journal of the American Academy of Orthopaedic Surgeons, 12*, 139–143. https://doi.org/10.5435/00124635-200405000-00001.

Davies, N. M., Røseth, A. G., Appleyard, C. B., McKnight, W., Del Soldato, P., Calignano, A., et al. (1997). NO-naproxen vs. naproxen: ulcerogenic, analgesic and anti-inflammatory effects. *Alimentary Pharmacology Therapeutics, 11,* 69–79.

Del Arco, M., Cebadera, E., Gutiérrez, S., Martín, C., Montero, M. J., Rives, V., Rocha, J., & Sevilla, M. A. (2004). Mg,Al layered double hydroxides with intercalated indomethacin: Synthesis, characterization, and pharmacological study. *Journal of Pharmaceutical Sciences, 93*, 1649–1658. https://doi.org/10.1002/jps.20054.

Djaballah, R., Bentouami, A., Benhamou, A., Boury, B., & Elandaloussi, E. H. (2018). The use of Zn-Ti layered double hydroxide interlayer spacing property for low-loading drug and low-dose therapy. Synthesis, characterization and release kinetics study. *Journal of Alloys and Compounds, 739*, 559–567. https://doi.org/10.1016/j.jallcom.2017.12.299.

Dresselhaus, M. S., editor (1986). *Intercalation in Layered Materials, 1st edition.* Springer, Berlin. https://doi.org/10.1007/978-1-4757-5556-5

Fayyazbakhsh, F., Solati-Hashjin, M., Keshtkar, A., Shokrgozar, M. A., Dehghan, M. M., & Larijani, B. (2017). Release behavior and signaling effect of vitamin D3 in layered double hydroxides-hydroxyapatite/gelatin bone tissue engineering scaffold: An in vitro evaluation. *Colloids and Surfaces B: Biointerfaces, 158*, 697–708. https://doi.org/10.1016/j.colsurfb.2017.07.004.

Hasan, Z., Jeon, J., & Jhung, S. H. (2012). Adsorptive removal of naproxen and clofibric acid from water using metal-organic frameworks. *Journal of Hazardous Materials, 209–210*, 151–157. https://doi.org/10.1016/j.jhazmat.2012.01.005.

Hines, D., Solin, S., Costantino, U., & Nocchetti, M. (2000). Physical properties of fixed-charge layer double hydroxides. *Physical Review B - Condensed Matter and Materials Physics, 61*, 11348–11358. https://doi.org/10.1103/PhysRevB.61.11348.

Hou, W., & Jin, Z. (2007). Synthesis and characterization of Naproxen intercalated Zn–Al layered double hydroxides. *Colloid and Polymer Science, 285*, 1449–1454. https://doi.org/10.1007/s00396-007-1704-y.

Huang, W., Zhang, H., & Pan, D. (2015). Study on the release behavior and mechanism by monitoring the morphology changes of the large-sized drug-LDH nanohybrids. *AIChE Journal, 6*, 857–866. https://doi.org/10.1002/aic.12379.

Hussein, A. M. A., Burra, K. G., Bassioni, G., Hammouda, R. M., & Gupta, A. K. (2019). Production of CO from CO_2 over mixed-metal oxides derived from layered. *Applied Energy, 235*(November 2018), 1183–1191. https://doi.org/10.1016/j.apenergy.2018.11.040.

Khan, A. I., Lei, L., & Norquist, A. J. (2001). Intercalation and controlled release of pharmaceutically active compounds from a layered double hydroxide. *Chemical Communications*, 2342–2343. https://doi.org/10.1039/b106465g

Kriven, W. M., Kwak, S., Wallig, M., & Choy, J. (2004). Bioresorbable nanoceramics for gene and drug. *MRS Bulletin, 2016*, 33–37. https://doi.org/10.1557/mrs2004.14.

Li, B., He, J., Evans, D. G., & Duan, X. (2004). Inorganic layered double hydroxides as a drug delivery system – Intercalation and in vitro release of fenbufen. *Applied Clay Science, 27*, 199–207. https://doi.org/10.1016/j.clay.2004.07.002.

Li, F., Jin, L., Han, J., Wei, M., & Li, C. (2009). Synthesis and controlled release properties of prednisone intercalated Mg-Al layered double hydroxide composite. *Industrial and Engineering Chemistry Research, 48,* 5590–5597. https://doi.org/10.1021/ie900043r.

Lichtenstein, D. R., Syngal, S., & Wolfe, M. (1995). Nonsteroidal antiinflammatory drugs and the gastrointestinal tract: The double-edged sword. *Arthritis & Rheumatism, 38*, 5–18.

Lobo, M. S., & Costa, P. (2001). Modeling and comparison of dissolution profiles´. *European Journal of Pharmaceutical Sciences, 13,* 123–133.

Menagen, B., Pedahzur, R., & Avnir, D. (2017). Sustained release from a metal – Analgesics entrapped within biocidal silver. *Scientific Reports, 7,* 1–11. https://doi.org/10.1038/s41598-017-03195-w.

Mishra, G., Dash, B., & Pandey, S. (2018). Layered double hydroxides: A brief review from fundamentals to application as evolving biomaterials. *Applied Clay Science, 153*, 172–186. https://doi.org/10.1016/j.clay.2017.12.021.

Mobbs, R. J., Coughlan, M., Thompson, R., Sutterlin, C. E., & Phan, K. (2017). The utility of 3D printing for surgical planning and patient-specific implant design for complex spinal pathologies: Case report. *Journal of Neurosurgery: Spine, 26*, 513–518. https://doi.org/10.3171/2016.9.SPINE16371.

Mondal, S., Dasgupta, S., & Maji, K. (2016). MgAl- Layered double hydroxide nanoparticles for controlled release of salicylate. *Materials Science and Engineering C, 68*, 557–564. https://doi.org/10.1016/j.msec.2016.06.029.

Mosmann, T. (1983). Rapid colorimetric assay for cellular growth and survival: Application to proliferation and cytotoxicity assays. *Journal of Immunological Methods, 65*, 55–63. https://doi.org/10.1016/0022-1759(83)90303-4.

Reichle, W. T. (1986). Synthesis of anionic clay minerals (mixed metal hydroxides, hydrotalcite). *Solid State Ionics, 22*, 135–141. https://doi.org/10.1016/0167-2738(86)90067-6.

Rhaese, S., Von Briesen, H., Rubsamen-waigmann, H., & Langer, K. (2003). H uman serum albumin – polyethylenimine nanoparticles for gene delivery. *Journal of Controlled Release, 92*, 199–208.

Richy, F., Bruyere, O., Ethgen, O., Rabenda, V., Bouvenot, G., Audran, M., & Reginster, J. Y. (2004). Time dependent risk of gastrointestinal complications induced by non-steroidal anti-inflammatory drug use: A consensus statement using a meta-analytic approach. *Annals of the Rheumatic Diseases, 63*(7), 759–766. https://doi.org/10.1136/ard.2003.015925.

Rives, V., Del Arco, M., & Martín, C. (2013). Layered double hydroxides as drug carriers and for controlled release of non-steroidal antiinflammatory drugs (NSAIDs): A review. *Journal of Controlled Release*, *169*, 28–39. https://doi.org/10.1016/j.jconrel.2013.03.034

Rojas, R., Jimenez-Kairuz, A. F., Manzo, R. H., & Giacomelli, C. E. (2014). Release kinetics from LDH-drug hybrids: Effect of layers stacking and drug solubility and polarity. *Colloids and Surfaces A: Physicochemical and Engineering Aspects, 463*, 37–43. https://doi.org/10.1016/j.colsurfa.2014.09.031.

Rojas, R., Linck, Y. G., Cuffini, S. L., Monti, G. A., & Giacomelli, C. E. (2015). Structural and physicochemical aspects of drug release from layered double hydroxides and layered hydroxide salts. *Applied Clay Science, 109–110*, 119–126. https://doi.org/10.1016/j.clay.2015.02.030.

Souza, J. M. F. d. S., de Aquino, A. L. F., & Basto, A. O. (2018). Treatment of heterotopic ossification of the hip with use of a plaster cast: case report. *Revista Brasileira de Ortopedia, 53*(6), 805–808. https://doi.org/10.1016/j.rbo.2017.05.012.

Tang, L., & Eaton, J. W. (1995). Inflammatory responses to biomaterials. *American Journal of Clinical Pathology, 4*, 466–471. https://doi.org/10.1093/ajcp/103.4.466.

Vielpeau, C., & Joubert, J. (1999). Naproxen in the prevention of heterotopic ossification after total hip replacement. *Clinical Orthopaedics and Related Research, 369*, 279–288.

Wei, M., Shi, S., Wang, J., Li, Y., & Duan, X. (2004). Studies on the intercalation of naproxen into layered double hydroxide and its thermal decomposition by in situ FT-IR and in situ HT-XRD. *Journal of Solid State Chemistry, 177*, 2534–2541. https://doi.org/10.1016/j.jssc.2004.03.041.

Xu, Z. P., Walker, T. L., Liu, K., Cooper, H. M., Lu, G. Q. M., & Bartlett, P. F. (2007). Layered double hydroxide nanoparticles as cellular delivery vectors of supercoiled plasmid DNA. *International Journal of Nanomedicine, 2*, 163–174. https://doi.org/10.2147/IJN.S.

Yang, K., Yan, L. G., Yang, Y. M., Yu, S. J., Shan, R. R., Yu, H. Q., & Du, B. (2014). Adsorptive removal of phosphate by Mg-Al and Zn-Al layered double hydroxides: Kinetics, isotherms and mechanisms. *Separation and Purification Technology, 124*, 36–42. https://doi.org/10.1016/j.seppur.2013.12.042.

(Received 15 May 2020; revised 11 September 2020; AE: Jin-Ho Choy)